Meccanica (2017) 52:251–262
DOI 10.1007/s11012-016-0393-3

An application of a size-dependent model on microplate with elastic medium based on strain gradient elasticity theory

Long Zhang · Binbin Liang · Shenjie Zhou · Binglei Wang · Yiguo Xue

Received: 27 January 2015 / Accepted: 12 February 2016 / Published online: 25 February 2016

Abstract A size-dependent Kirchhoff micro-plate model resting on elastic medium is developed based on the strain gradient elasticity theory. Three material length scale parameters are introduced in the model, and those parameters may effectively capture the size effect. The model can degenerate into the modified couple stress plate model or the classical plate model by setting two (l_0 and l_1) or all (l_0, l_1 and l_2) of the material length scale parameters to be zero. Analytical solutions for the static bending, buckling and free vibration problems of a rectangular micro-plate with all edges simply supported are obtained. The results predicted by the present model are compared with those predicted by the degraded models. Influences of the elastic medium on the static bending, buckling, and free vibration are discussed. The results show that the present model can predict prominent size-dependent normalized stiffness, buckling load, and natural frequency with the reduction of structural size, especially when the plate thickness is on the same order of the material length scale parameter. The study may be helpful to guide the design of microplate-based devices resting on elastic medium for a wide range of potential applications.

Keywords Micro plates · Elastic medium · Size effect · Strain gradient elasticity theory

L. Zhang · B. Liang · B. Wang (✉) · Y. Xue
School of Civil Engineering, Shandong University, Jinan 250061, China
e-mail: bwang@sdu.edu.cn

S. Zhou
School of Mechanical Engineering, Shandong University, Jinan 250061, China

B. Wang
State Key Laboratory for Strength and Vibration of Mechanical Structures, School of Aerospace, Xi'an Jiaotong University, Xi'an 710049, China

1 Introduction

With the development of recent technology, opportunities of promising research and engineering priorities in micro-plate have been opened up based on micromechanics [1], where the thickness of plates is typically on the order of microns or sub-microns. The size-dependent behavior of micro scale structures has been verified experimentally in some kinds of materials [2–8]. Hence, the size effect must be taken into account in studies of micro scale structures.

However, the classical theory of linear elasticity does not involve the size effect in micro scale structures. Recently, many scientists [3, 6, 8–15] have done some work based on higher-order continuum theories, in which strain gradient or non-local terms are involved and additional material length scale parameters are introduced in addition to the classical material constants. Several micro-plate models have been developed by many researchers based on some higher-order continuum theories, e.g., micropolar theory [16, 17], the simplest version of the simplified form-II theory of strain gradient linear elasticity [15, 18–20], gradient elastic theory [21, 22], and couple stress theory [23–25]. Ariman [16, 17] studied the circular micropolar plate and discussed some problems of the model. According to the gradient elasticity theory proposed by Altan and Aifantis [26–29], a gradient elasticity theory of plates is established by Lazopoulos [21]. And the gradient elasticity theory can be traced back to Mindlin [30]. Lazopoulos [22] considered the bending problem of strain gradient elastic thin plates by using a simple version of Mindlin's linear theory of elasticity with microstructure. In addition to the classical Lame constants, the intrinsic bulk length g and the directional surface energy length l_k are introduced in this theory for characterizing the strain gradient. Tsiatas [25] studied the static problem of a micro Kirchhoff plate with arbitrary shape based on the simplified couple stress theory proposed by Yang et al. [31].

The couple stress theory [32], a general form of the modified couple stress theory [31], was used by Tsiatas [25] to capture the size effect of micro-plate. It was pointed out by Shu and Fleck [33] that it usually under-predicts the size effect because the couple stress theory only employs the rotation gradient and neglects the other gradients (e.g. stretch gradient). Therefore, in order to account for the size effect more effectively, a general strain gradient theory should be introduced, which employs not only the rotation gradient but also stretch gradient or other gradients.

The strain gradient elasticity theory proposed by Lam et al. [8] contains three material length scale parameters and can be successfully applied to predict the size-dependent properties for small scale structures. This theory has been used to analyze the static and dynamic problems of micro scale Bernoulli–Euler beam [14], Timoshenko beam [12] and Kirchhoff plate [34]. Moreover, the strain gradient elasticity theory [8] can degenerate into the modified couple stress theory [31] by setting two of the three material length scale parameters to zero; thus, the modified couple stress theory [31] may be regarded as a special case of the strain gradient elasticity theory [8].

Some works [35–39] have been conducted to study the vibration and bending analysis of plates on elastic foundation based on the classical continuum elasticity. Recently, Akgoz and Caivalek [40] modeled and analyzed the micro plate resting on elastic foundation using the modified couple stress theory. Influences of the elastic medium and the length scale parameter on the bending, buckling, and vibration properties are discussed. Since the modified couple stress theory is a special case of the strain gradient elasticity theory, the micro plate model resting on elastic medium based on strain gradient elasticity theory is necessary to be discussed, which, to the best knowledge of authors, has not been studied in the literature.

In this study, an application of a size-dependent Kirchhoff micro-plate model resting on elastic medium is presented based on the strain gradient elasticity theory [8]. In Sect. 2, the governing equation and boundary conditions of the size-dependent Kirchhoff micro-plate model embedded in elastic medium are derived. In subsequent Sects. 3, 4 and 5, static bending, buckling and free vibration analyses of the simply supported plate resting on elastic medium are described and discussed. Conclusions are summarized in Sect. 6.

2 The size-dependent model for micro-sized plates resting on elastic medium

According to the strain gradient theory proposed by Lam et al. [8], in addition to two classical material constants, three independent material length scale parameters (MLSPs) are introduced for isotropic linear elastic materials. Then the strain energy U for the isotropic linear elastic material occupying region Ω is written as

$$U = \frac{1}{2}\int_{\Omega} \bar{u} d\Omega = \frac{1}{2}\iiint_{\Omega} \bar{u} dxdydz \tag{1}$$

where $\bar{u}$ is the strain energy density, defined as

$$\bar{u} = \sigma_{ij}\varepsilon_{ij} + p_i\gamma_i + \tau^{(1)}_{ijk}\eta^{(1)}_{ijk} + m^s_{ij}\chi^s_{ij} \tag{2}$$

in which ε_{ij} is the strain tensor, γ_i is the dilatation gradient tensor, $\eta^{(1)}_{ijk}$ is the deviatoric stretch gradient tensor, and χ^s_{ij} is the symmetric rotation gradient tensor, defined as

$$\varepsilon_{ij} = \frac{1}{2}(u_{i,j} + u_{j,i}) \tag{3}$$

$$\gamma_i = \varepsilon_{mm,i} \tag{4}$$

$$\eta^{(1)}_{ijk} = \eta^s_{ijk} - \frac{1}{5}(\delta_{ij}\eta^s_{mmk} + \delta_{jk}\eta^s_{mmi} + \delta_{ki}\eta^s_{mmj}) \tag{5}$$

$$\chi_{ij}^{s}=\frac{1}{2}\left(e_{ipq}\varepsilon_{qj,p}+e_{jpq}\varepsilon_{qi,p}\right)\tag{6}$$

where u_i is the displacement vector, ε_{mm} is the dilatation strain, δ_{ij} and e_{ijk} are the Knocker symbol and the alternate symbol respectively, and η_{ijk}^{s} is the symmetric part of second-order displacement gradient tensor, given by

$$\eta_{ijk}^{s}=\frac{1}{3}\left(u_{i,jk}+u_{j,ki}+u_{k,ij}\right)\tag{7}$$

Here it should be noted that the index notation will always be used with repeated indices denoting summation from 1 to 3.

The corresponding stress measures, respectively, are given by the following constitutive relations,

$$\sigma_{ij}=\lambda\delta_{ij}\varepsilon_{mm}+2\mu\varepsilon_{ij}\tag{8}$$

$$p_i=2\mu l_0^2\gamma_i\tag{9}$$

$$\tau_{ijk}^{(1)}=2\mu l_1^2\eta_{ijk}^{(1)}\tag{10}$$

$$m_{ij}^{s}=2\mu l_2^2\chi_{ij}^{s}\tag{11}$$

In the above equations, l_0, l_1 and l_2 are the additional independent MLSPs associated with the dilatation gradients, deviatoric stretch gradients and symmetric rotation gradients, respectively. The parameters λ and μ in the constitutive equation of the classical stress σ_{ij} denote the bulk and shear moduli respectively and can be written in terms of the Young modulus E and the Poisson's ratio v as

$$\lambda=\frac{Ev}{(1+v)(1-2v)}\ ,\quad \mu=\frac{E}{2(1+v)}\tag{12}$$

Consider an initially flat thin rectangular micro-plate embedded in elastic medium, as shown in Fig. 1. The plate is subject to a static transverse load $q(x, y)$ distributed in the $x-y$ plane. k is the elastic foundation parameter. The plate is assumed to be made by homogeneous linearly elastic material. According to Kirchhoff's plate theory, the displacement field can be defined as

$$\begin{aligned}u_x(x,y,z)&=-z\frac{\partial w(x,y)}{\partial x}\\ u_y(x,y,z)&=-z\frac{\partial w(x,y)}{\partial y}\\ u_z(x,y,z)&=w(x,y)\end{aligned}\tag{13}$$

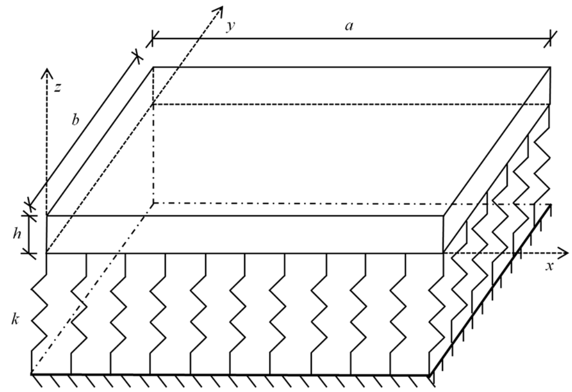

Fig. 1 Geometry and coordinates of a thin rectangular micro-plate model on an elastic medium

where $u_i(x,y,z)(i=x,\,y,\,z)$ are displacement components along x, y, z directions.

Substituting Eq. (13) into Eq. (3), the nonzero components of the strain tensor are written as

$$\varepsilon_{11}=-z\frac{\partial^2 w}{\partial x^2};\quad \varepsilon_{22}=-z\frac{\partial^2 w}{\partial y^2};\quad \varepsilon_{12}=-z\frac{\partial^2 w}{\partial x\partial y}\tag{14}$$

By using Eqs. (4) and (14), the non-zero components of the dilatation gradient tensor γ_i can be achieved

$$\gamma_1=-z\left(\frac{\partial^3 w}{\partial x^3}+\frac{\partial^3 w}{\partial x\partial y^2}\right);\quad \gamma_2=-z\left(\frac{\partial^3 w}{\partial y^3}+\frac{\partial^3 w}{\partial x^2\partial y}\right);\quad \gamma_3=-\left(\frac{\partial^2 w}{\partial x^2}+\frac{\partial^2 w}{\partial y^2}\right)\tag{15}$$

By inserting Eqs. (14) into (6), the non-zero components of the symmetric rotation gradient χ_{ij}^{s} are

$$\chi_{11}^{s}=\frac{\partial^2 w}{\partial x\partial y};\quad \chi_{22}^{s}=-\frac{\partial^2 w}{\partial x\partial y};\quad \chi_{12}^{s}=\frac{1}{2}\left(\frac{\partial^2 w}{\partial y^2}-\frac{\partial^2 w}{\partial x^2}\right)\tag{16}$$

From Eqs. (5), (7) and (13), the non-zero components of the deviatoric stretch gradient $\eta_{ijk}^{(1)}$ are

$$\begin{aligned}\eta_{111}^{(1)}&=\frac{1}{5}z\left(3\frac{\partial^3 w}{\partial x\partial y^2}-2\frac{\partial^3 w}{\partial x^3}\right);\\ \eta_{222}^{(1)}&=\frac{1}{5}z\left(3\frac{\partial^3 w}{\partial x^2\partial y}-2\frac{\partial^3 w}{\partial y^3}\right)\\ \eta_{333}^{(1)}&=\frac{1}{5}\left(\frac{\partial^2 w}{\partial x^2}+\frac{\partial^2 w}{\partial y^2}\right);\end{aligned}$$

$$\begin{aligned}\eta_{112}^{(1)} &= \eta_{121}^{(1)} = \eta_{211}^{(1)} = \frac{1}{5}z\left(\frac{\partial^3 w}{\partial y^3} - 4\frac{\partial^3 w}{\partial x^2 \partial y}\right)\eta_{113}^{(1)} \\ &= \eta_{131}^{(1)} = \eta_{311}^{(1)} = \frac{1}{15}\left(\frac{\partial^2 w}{\partial y^2} - 4\frac{\partial^2 w}{\partial x^2}\right)\eta_{221}^{(1)} \\ &= \eta_{212}^{(1)} = \eta_{122}^{(1)} = \frac{1}{5}z\left(\frac{\partial^3 w}{\partial x^3} - 4\frac{\partial^3 w}{\partial x \partial y^2}\right)\eta_{223}^{(1)} \\ &= \eta_{232}^{(1)} = \eta_{322}^{(1)} = \frac{1}{15}\left(\frac{\partial^2 w}{\partial x^2} - 4\frac{\partial^3 w}{\partial y^2}\right)\eta_{331}^{(1)} \\ &= \eta_{313}^{(1)} = \eta_{133}^{(1)} = \frac{1}{5}z\left(\frac{\partial^3 w}{\partial x^3} + \frac{\partial^3 w}{\partial x \partial y^2}\right)\eta_{332}^{(1)} \\ &= \eta_{323}^{(1)} = \eta_{233}^{(1)} = \frac{1}{5}z\left(\frac{\partial^3 w}{\partial y^3} + \frac{\partial^3 w}{\partial x^2 \partial y}\right)\eta_{123}^{(1)} \\ &= \eta_{231}^{(1)} = \eta_{312}^{(1)} = \eta_{123}^{(1)} = \eta_{213}^{(1)} = \eta_{321}^{(1)} = \frac{1}{3}\frac{\partial^2 w}{\partial x \partial y}\end{aligned} \tag{17}$$

It is worth noting that the present model is a plane stress problem, according to elasticity mechanics, the classical stress of the present model can be obtained by

$$\sigma_{ij} = \frac{Ev}{1 - v^2}\delta_{ij}\varepsilon_{mm} + \frac{E}{1 + v}\varepsilon_{ij} \tag{18}$$

Finally, by inserting the strain tensors into Eqs. (9), (10), (11) and (18), the stress tensors can be obtained. When the strain and stress tensors are substituted into Eq. (2), the strain energy density $\bar{u}$ is obtained by taking somewhat lengthy but straightforward manipulation:

$$\begin{aligned}\bar{u} = &(c_1 + c_2 z^2)\left(\left(\frac{\partial^2 w}{\partial x^2}\right)^2 + \left(\frac{\partial^2 w}{\partial y^2}\right)^2\right) \\ &+ (c_3 + c_4 z^2)\left(\frac{\partial^2 w}{\partial x^2}\frac{\partial^2 w}{\partial y^2}\right) \\ &+ (c_5 + c_6 z^2)\left(\frac{\partial^2 w}{\partial x \partial y}\right)^2 + c_7 z^2\left(\left(\frac{\partial^3 w}{\partial x^3}\right)^2 + \left(\frac{\partial^3 w}{\partial y^3}\right)^2\right) \\ &+ c_8 z^2\left(\left(\frac{\partial^3 w}{\partial x \partial y^2}\right)^2 + \left(\frac{\partial^3 w}{\partial x^2 \partial y}\right)^2\right) \\ &+ c_9 z^2\left(\frac{\partial^3 w}{\partial x^3}\frac{\partial^3 w}{\partial x \partial y^2} + \frac{\partial^3 w}{\partial y^3}\frac{\partial^3 w}{\partial x^2 \partial y}\right)\end{aligned} \tag{19}$$

in which

$$\begin{aligned}&c_1 = 2\mu l_0^2 + \frac{8}{15}\mu l_1^2 + \mu l_2^2; \quad c_2 = \frac{E}{1 - v^2}; \\ &c_3 = 4\mu l_0^2 - \frac{4}{15}\mu l_1^2 - 2\mu l_2^2 \\ &c_4 = \frac{2Ev}{1 - v^2}; \quad c_5 = \frac{4}{3}\mu l_1^2 + 4\mu l_2^2; \quad c_6 = 4\mu \\ &c_7 = 2\mu l_0^2 + \frac{4}{5}\mu l_1^2; \quad c_8 = 2\mu l_0^2 + \frac{24}{5}\mu l_1^2; \\ &c_9 = 4\mu l_0^2 - \frac{12}{5}\mu l_1^2\end{aligned} \tag{20}$$

We assume the following integral relations,

$$\begin{aligned}&\iiint_V z^2 dxdydz = I\iint_A dxdy \qquad I = \int_{-\frac{h}{2}}^{\frac{h}{2}} z^2 dz = \frac{h^3}{12} \\ &\iiint_V dxdydz = h\iint_A dxdy\end{aligned} \tag{21}$$

Substituting Eq. (19) into Eq. (1), and the variation of strain energy can be obtained as

$$\begin{aligned}\delta U = &\iiint_V \delta\bar{u}dxdydz = \iint_S \delta F dxdy \\ = &\iint_S \left(\left(\frac{\partial F}{\partial w_{xx}}\right)\delta w_{xx} + \left(\frac{\partial F}{\partial w_{yy}}\right)\delta w_{yy}\right. \\ &+ \left(\frac{\partial F}{\partial w_{xy}}\right)\delta w_{xy} + \left(\frac{\partial F}{\partial w_{xxx}}\right)\delta w_{xxx} \\ &+ \left(\frac{\partial F}{\partial w_{yyy}}\right)\delta w_{yyy} + \left(\frac{\partial F}{\partial w_{xyy}}\right)\delta w_{xyy} \\ &\left.+ \left(\frac{\partial F}{\partial w_{xxy}}\right)\delta w_{xxy}\right)dxdy\end{aligned} \tag{22}$$

where

$$\begin{aligned}F = &(c_1 h + c_2 I)\left(\left(\frac{\partial^2 w}{\partial x^2}\right)^2 + \left(\frac{\partial^2 w}{\partial y^2}\right)^2\right) \\ &+ (c_3 h + c_4 I)\left(\frac{\partial^2 w}{\partial x^2}\frac{\partial^2 w}{\partial y^2}\right) + (c_5 h + c_6 I)\left(\frac{\partial^2 w}{\partial x \partial y}\right)^2 \\ &+ c_7 I\left(\left(\frac{\partial^3 w}{\partial x^3}\right)^2 + \left(\frac{\partial^3 w}{\partial y^3}\right)^2\right) + c_8 I\left(\left(\frac{\partial^3 w}{\partial x \partial y^2}\right)^2\right. \\ &\left.+ \left(\frac{\partial^3 w}{\partial x^2 \partial y}\right)^2\right) + c_9 I\left(\frac{\partial^3 w}{\partial x^3}\frac{\partial^3 w}{\partial x \partial y^2} + \frac{\partial^3 w}{\partial y^3}\frac{\partial^3 w}{\partial x^2 \partial y}\right)\end{aligned} \tag{23}$$

and

$$w_{xx} = \frac{\partial^2 w}{\partial x^2}; \quad w_{yy} = \frac{\partial^2 w}{\partial y^2}; \quad w_{xy} = \frac{\partial^2 w}{\partial x \partial y}$$
$$w_{xxx} = \frac{\partial^3 w}{\partial x^3}; \quad w_{yyy} = \frac{\partial^3 w}{\partial y^3}; \quad w_{xxy} = \frac{\partial^3 w}{\partial x^2 \partial y};$$
$$w_{xyy} = \frac{\partial^3 w}{\partial x \partial y^2} \tag{24}$$

By applying the rules of integration by parts, Eq. (22) is rewritten as

$$\begin{aligned}
\delta U = & \iint \left(\frac{\partial^2}{\partial x^2}\left(\frac{\partial F}{\partial w_{xx}}\right) + \frac{\partial^2}{\partial y^2}\left(\frac{\partial F}{\partial w_{yy}}\right) + \frac{\partial^2}{\partial x \partial y}\left(\frac{\partial F}{\partial w_{xy}}\right) \right.\\
& - \frac{\partial^3}{\partial x^3}\left(\frac{\partial F}{\partial w_{xxx}}\right) - \frac{\partial^3}{\partial y^3}\left(\frac{\partial F}{\partial w_{yyy}}\right).\\
& \left. - \frac{\partial^3}{\partial x \partial y^2}\left(\frac{\partial F}{\partial w_{xyy}}\right) - \frac{\partial^3}{\partial x^2 \partial y}\left(\frac{\partial F}{\partial w_{xxy}}\right) \right) \delta w dx dy\\
& + \int \left(\left(-\frac{\partial}{\partial y}\left(\frac{\partial F}{\partial w_{yy}}\right) - \frac{\partial}{\partial x}\left(\frac{\partial F}{\partial w_{xy}}\right) + \frac{\partial^2}{\partial y^2}\left(\frac{\partial F}{\partial w_{yyy}}\right) \right.\right.\\
& + \frac{\partial^2}{\partial x \partial y}\left(\frac{\partial F}{\partial w_{xyy}}\right) + \frac{\partial^2}{\partial x^2}\left(\frac{\partial F}{\partial w_{xxy}}\right)) \delta w.\\
& + \left(\frac{\partial F}{\partial w_{yy}} - \frac{\partial}{\partial y}\left(\frac{\partial F}{\partial w_{yyy}}\right) - \frac{\partial}{\partial x}\left(\frac{\partial F}{\partial w_{xyy}}\right) \right) \delta w_y\\
& + \frac{\partial F}{\partial w_{yyy}} \delta w_{yy}) |_0^b dx \quad + \int \left(\left(-\frac{\partial}{\partial x}\left(\frac{\partial F}{\partial w_{xx}}\right) \right.\right.\\
& - \frac{\partial}{\partial y}\left(\frac{\partial F}{\partial w_{xy}}\right) + \frac{\partial^2}{\partial x^2}\left(\frac{\partial F}{\partial w_{xxx}}\right)\\
& + \frac{\partial^2}{\partial x \partial y}\left(\frac{\partial F}{\partial w_{xxy}}\right) + \frac{\partial^2}{\partial y^2}\left(\frac{\partial F}{\partial w_{xyy}}\right)) \delta w.\\
& + \left(\frac{\partial F}{\partial w_{xx}} - \frac{\partial}{\partial x}\left(\frac{\partial F}{\partial w_{xxx}}\right) - \frac{\partial}{\partial y}\left(\frac{\partial F}{\partial w_{xxy}}\right) \right) \delta w_x\\
& \left. + \frac{\partial F}{\partial w_{xxx}} \delta w_{xx} \right) |_0^a dy
\end{aligned} \tag{25}$$

The first variation of the virtual work done by external loads can be rewritten as

$$\delta W = \iint_S [q(x,y) - kw(x,y)] \delta w(x,y) dx dy \tag{26}$$

in which $q(x,y)$ is the distributed transverse load on the plate and k is the elastic foundation parameter.

Then, Eqs. (25) and (26) are substituted into the following expression of principle of minimum potential energy

$$\delta(U - W) = 0 \tag{27}$$

Due to the variational principle for arbitrary δw, the governing equation is finally obtained by taking somewhat lengthy but straightforward manipulations:

$$-p_1 \nabla^6 w + p_2 \nabla^4 w + kw = q(x,y) \tag{28}$$

where

$$\begin{aligned}
p_1 &= \mu I (2l_0^2 + \frac{4}{5} l_1^2)\\
p_2 &= \mu h (2l_0^2 + \frac{8}{15} l_1^2 + l_2^2) + \frac{E}{1 - \nu^2} I
\end{aligned} \tag{29}$$

and

$$\begin{aligned}
\nabla^6 w &= \frac{\partial^6 w}{\partial x^6} + 3\frac{\partial^6 w}{\partial x^2 \partial y^4} + 3\frac{\partial^6 w}{\partial x^4 \partial y^2} + \frac{\partial^6 w}{\partial y^6}\\
\nabla^4 w &= \frac{\partial^4 w}{\partial x^4} + 2\frac{\partial^4 w}{\partial x^2 \partial y^2} + \frac{\partial^4 w}{\partial y^4}
\end{aligned} \tag{30}$$

The corresponding exact boundary conditions at the edges can also be obtained:

$$\begin{aligned}
& B_{X1}(a,y)\delta w(a,y) - B_{X1}(0,y)\delta w(0,y) = 0\\
& B_{X2}(a,y)\delta w_x(a,y) - B_{X2}(0,y)\delta w_x(0,y) = 0\\
& B_{X3}(a,y)\delta w_{xx}(a,y) - B_{X3}(0,y)\delta w_{xx}(0,y) = 0\\
& B_{Y1}(x,b)\delta w(x,b) - B_{Y1}(x,0)\delta w(x,0) = 0\\
& B_{Y2}(x,b)\delta w_y(x,b) - B_{Y2}(x,0)\delta w_y(x,0) = 0\\
& B_{Y3}(x,b)\delta w_{yy}(x,b) - B_{Y3}(x,0)\delta w_{yy}(x,0) = 0
\end{aligned} \tag{31}$$

in which

$$\begin{aligned}
& B_{X1}(x,y) = -2P_1 \frac{\partial^3 w}{\partial x^3} + 2P_4 \frac{\partial^5 w}{\partial x^5};\\
& B_{X2}(x,y) = 2P_1 \frac{\partial^2 w}{\partial x^2} - 2P_4 \frac{\partial^4 w}{\partial x^4}\\
& B_{X3}(x,y) = 2P_4 \frac{\partial^3 w}{\partial x^3};\\
& B_{Y1}(x,y) = -2P_1 \frac{\partial^3 w}{\partial y^3} + 2P_4 \frac{\partial^5 w}{\partial y^5}\\
& B_{Y2}(x,y) = 2P_1 \frac{\partial^2 w}{\partial y^2} - 2P_4 \frac{\partial^4 w}{\partial y^4};\\
& B_{Y3}(x,y) = 2P_4 \frac{\partial^3 w}{\partial y^3}
\end{aligned} \tag{32}$$

and

$$P_1 = c_1 h + c_2 I \quad P_2 = c_3 h + c_2 I \quad P_3 = c_5 h + c_6 I$$
$$P_4 = c_7 I \qquad P_5 = c_8 I \qquad P_6 = c_9 I \tag{33}$$

3 Static bending of simply supported size-dependent plate

Firstly, to illustrate the present model, the static bending problem of a rectangular micro-plate with all edges simply supported is considered. The micro-plate is subject to a lateral uniformly distributed load $q(x, y)$ and a lateral reaction force $kw(x, y)$ due to elastic medium.

It is noted that based on the principal of variation [41], the boundary conditions can be classified to two groups: kinematic boundary conditions and natural boundary conditions. The boundary conditions are determined by specifying the kinematic boundary conditions or by satisfying the natural boundary conditions. For the boundary conditions given in Eq. (31), the kinematic and natural boundary condition are given as follows

$$\begin{array}{l} \textit{Kinematic} \quad \textit{natural} \\ \left.\begin{array}{lll} B_{X1}=0 & or & w=0 \\ B_{X2}=0 & or & w_{,x}=0 \\ B_{X3}=0 & or & w_{,xx}=0 \end{array}\right\} \; for\ x=0,\ a \\ \left.\begin{array}{lll} B_{Y1}=0 & or & w=0 \\ B_{Y2}=0 & or & w_{,y}=0 \\ B_{Y3}=0 & or & w_{,yy}=0 \end{array}\right\} \; for\ y=0,\ b \end{array} \tag{34}$$

The classical boundary conditions for the simply supported plate are

$$\begin{array}{l} w=0,\ B_{X2}=0 \quad for \quad x=0,\ a \\ w=0,\ B_{Y2}=0 \quad for \quad y=0,\ b \end{array} \tag{35}$$

Similar to our previous work [14], for non-classical boundary conditions, there are two possible boundary conditions at both ends:

$$\begin{array}{l} w_{xx}(x,y)=0\ for\ x=0,\ a \\ w_{yy}(x,y)=0\ for\ y=0,\ b \end{array} \quad \text{or} \quad \begin{array}{l} B_{X3}(x,y)=0\ for\ x=0,\ a \\ B_{Y3}(x,y)=0\ for\ y=0,\ b \end{array} \tag{36}$$

For illustration purposes, here, the boundary conditions for the simply supported plate are selected as

$$\begin{array}{l} \left.\begin{array}{l} w(x,y)=0 \\ B_{X2}(x,y)=0 \\ w_{xx}(x,y)=0 \end{array}\right\} \; for\ x=0,\ a \\ \left.\begin{array}{l} w(x,y)=0 \\ B_{Y2}(x,y)=0 \\ w_{yy}(x,y)=0 \end{array}\right\} \; for\ y=0,\ b \end{array} \tag{37}$$

In order to solve the governing Eq. (28) with the boundary conditions in Eq. (37), the following Fourier series $w(x, y)$ is assumed:

$$w(x,y) = \sum_{m=1}^{\infty}\sum_{n=1}^{\infty} A_{mn} \sin\left(\frac{m\pi x}{a}\right) \sin\left(\frac{n\pi y}{b}\right) \tag{38}$$

where A_{mn} is the Fourier coefficient. It is obvious that Eq. (38) satisfies the corresponding boundary conditions in Eq. (37). Similarly, the lateral uniformly distributed load $q(x, y)$ can also be expressed as Fourier series:

$$q(x,y) = \sum_{m=1}^{\infty}\sum_{n=1}^{\infty} Q_{mn} \sin\left(\frac{m\pi x}{a}\right) \sin\left(\frac{n\pi y}{b}\right) \tag{39}$$

In the case of the uniformly distributed load $q(x, y) = q_0$, Q_{mn} is expressed as [13]

$$Q_{mn} = \frac{16 q_0}{mn\pi^2} \quad m, n = 1, 3, 5\ldots \tag{40}$$

Substituting Eqs. (38) and (39) into Eq. (28), A_{mn} can be calculated as

$$A_{mn} = \frac{Q_{mn}}{C_1 p_1 + C_2 p_2 + k} \tag{41}$$

in which

$$\begin{array}{l} C_1 = \left(\left(\frac{m\pi}{a}\right)^2 + \left(\frac{n\pi}{b}\right)^2\right)^3 \\ C_2 = \left(\left(\frac{m\pi}{a}\right)^2 + \left(\frac{n\pi}{b}\right)^2\right)^2 \end{array} \tag{42}$$

For simplification, it is assumed that all three MLSPs are the same, i.e. $l_0 = l_1 = l_2 = Cl$. For the purpose of illustration, unless otherwise stated, the plate considered here has the following properties: the elastic modulus $E = 1.44$ GPa, Poisson's ratio $v = 0.3$, the material length scale parameter

$Cl = 4.0\ \mu m$, the aspect ratio of the plate to be the same, i.e., $a/h = 50$, $b/h = 50$. The thickness of the plate $h = f{\cdot}Cl$, in which f is the dimensionless size scale. The lateral uniformly distributed load $q = 0.1\ \mu N/\mu m^2$, and the density of the plate $\rho = 1220\ kg/m^3$.

Figure 2 shows the variation of the normalized micro-plate stiffness (h/w_{max}) with the size scale (f), where w_{max} is the deflection of the plate at the central point ($x = a/2$, $y = b/2$). Results predicted by the present model are compared with those predicted by the modified couple stress model [40] and the classical model [42]. As shown in Fig. 2, when the plate is not affected by the elastic medium($k = 0$), the normalized stiffness keeps constant for the classical model, while for the present model and the modified couple stress model, the normalized stiffness decreases nonlinearly as the size scale increases. These three models show almost no difference of the normalized stiffness if the plate thickness is more than 15 times larger than the material length scale parameter; while with a smaller size scale (i.e., smaller plate dimension for the same material) the present model shows strong size effect, and that leads to a higher normalized stiffness. When the elastic medium (assuming $k = 10^9 Pa/m$) is considered, the normalized stiffness increases almost linearly for the classical model, while for the present model and the modified couple stress model, the normalized stiffness decreases and then increases as the size scale increases. And when the plate thickness is more than 15 times larger than the material length scale parameter, the three models show almost no difference of the normalized stiffness; while with a smaller size scale the present model shows strong size effect.

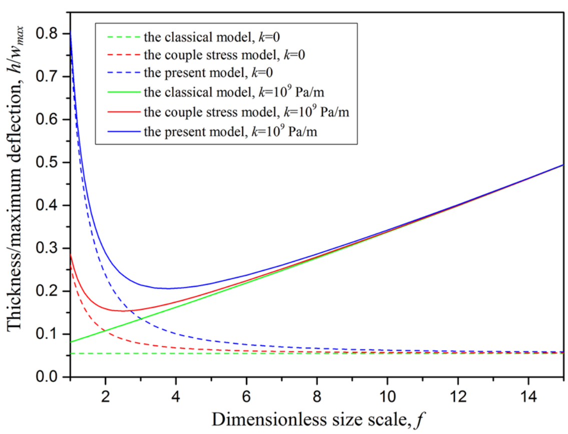

Fig. 2 Normalized stiffness with size scale

Figure 3 shows the change of the maximum deflection with foundation parameter for all of the three models. As shown in Fig. 3, the results from the three models are quite different, and the size-dependent phenomenon is significantly pronounced when k is less than $10^{11} Pa/m$. The maximum deflections predicted by the present model and by the couple stress model are about 13.6 and 4.6 times of that obtained by the classical model for $k = 10^8\ Pa/m$. When the foundation parameter k is greater than $10^{11} Pa/m$,the maximum deflections of the plate predicted by the three model are almost the same. So the size effect of

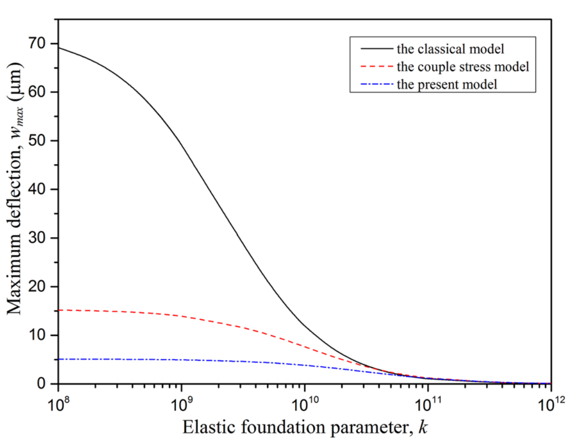

Fig. 3 Variation of the maximum plate deflection with foundation parameters

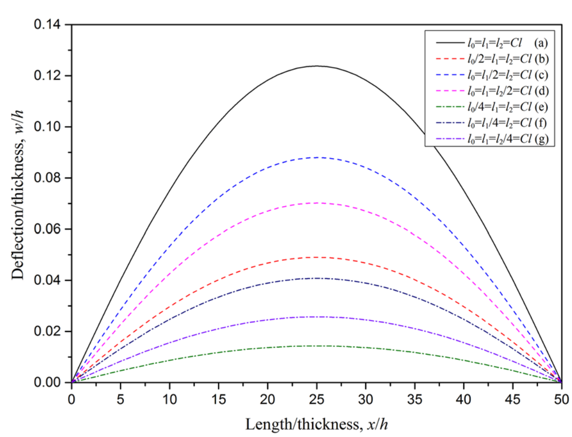

Fig. 4 Effects of different MLSPs on deflection

the micro-plate is significant and cannot be neglected when the foundation parameter k is smaller than $10^{11} Pa/m$.

In the present model, three MLSPs are incorporated corresponding to the three strain gradient tensors (the dilatation gradient, the deviatoric stretch gradient and the symmetric rotation gradient). The MLSPs, however, are assumed to be the same value in Figs. 2 and 3, i.e., $l_0 = l_1 = l_2 = Cl$. In order to study the role of each strain gradient tensor in the present model, the deflection of the plate at the central line ($y = b/2$) with different cases for MLSPs are presented in Fig. 4, where the results of: (a) $l_0 = l_1 = l_2 = Cl$, (b) $l_0/2 = l_1 = l_2 = Cl$, (c) $l_0 = l_1/2 = l_2 = Cl$, (d) $l_0 = l_1 = l_2/2 = Cl$, (e) $l_0/4 = l_1 = l_2 = Cl$, (f) $l_0 = l_1/4 = l_2 = Cl$, (g) $l_0 = l_1 = l_2/4 = Cl$ are given and compared. Here, the lateral uniformly distributed load $q = 0.01\ \mu N/\mu m^2$, and the other parameters are the same as those given before. Of course, the dimensionless deflections of case (b)–(d) are smaller than that of case (a) as case (b)–(d) use double values of l_0, l_1, l_2, respectively, compared to case (a). It is shown that the results of case (d) are smaller than those of case (c) but larger than those of case (b), indicating that the symmetric rotation gradient plays less role than the dilatation gradient and plays more important role than the deviatoric stretch gradient in the present model. The results of (e)–(g) are smaller than the results of (a)–(d) as $4Cl$ is substituted into l_0, l_1, l_2 in (e)–(g), respectively. Furthermore, from another point of view, the deflection reduces with l_0/l_1 increasing if we compare results of (a), (b), (e) (i.e., l_1/l_2 fixed, $l_0/l_1 = 1, 2, 4$, respectively). The same tendencies are also found when comparing (a), (c), (f) or (a), (d), (g). Again, here, it is shown that l_0 is more sensitive than l_1 and l_2, and l_1 is the least sensitive among the three MLSPs, which indeed affect the resultant strain gradient effect more or less by altering these ratios among MLSPs. The similar conclusions are also drawn in Ref. [43], where different material characteristic lengths are studied and discussed respectively to evaluate the optimal structure. This may guide us to pay more attention on the dilation gradient in determining MLSPs. It is noted that the MLSPs are internal parameters of a given material, and in practice, they are generally different and determined by uniaxial tensile, torsional or bending experiments for different size.

4 Stability analysis of simply supported size-dependent plate

Secondly, stability analysis of a simply supported rectangular micro-plate on an elastic foundation is considered. In addition to a lateral distributed load $q(x, y)$ and a lateral reaction force $kw(x, y)$ due to elastic medium, the micro-plate is also subject to in-plane compressive loads $\boldsymbol{P} = (P_x, P_{xy}, P_y)$, P_x and P_y are the load along x-axis direction and y-axis direction respectively, P_{xy} is the shear load in the x–y plane. According to the classical theory, there exists a critical buckling load P_{cr}. The governing equation is given as

$$-p_1\nabla^6 w + p_2\nabla^4 w + +P_x\frac{\partial^2 w}{\partial x^2} + 2P_{xy}\frac{\partial^2 w}{\partial x\partial y} + P_y\frac{\partial^2 w}{\partial y^2} + kw = q(x,y) \tag{43}$$

The boundary conditions are expressed in Eq. (37).

In order to simplify analysis, P_x and $kw(x, y)$ are only considered, the other loads are set to zero. So Eq. (43) can be rewritten as

$$-p_1\nabla^6 w + p_2\nabla^4 w + P_x\frac{\partial^2 w}{\partial x^2} + kw = 0 \tag{44}$$

The following Fourier series is also used for this problem,

$$w(x,y) = \sum_{m=1}^{\infty}\sum_{n=1}^{\infty} B_{mn}\sin(\frac{m\pi x}{a})\sin(\frac{n\pi y}{b}) \tag{45}$$

By substituting Eq. (45) into Eq. (44), it is obtained as

$$P_x = \frac{C_1p_1 + C_2p_2 + k}{(\frac{m\pi}{a})^2} \tag{46}$$

The critical buckling load P_{cr} is equal to the minimum of P_x in Eq. (46). The critical buckling load P_{cr} can be obtained by setting $m = 1$ and $n = 1$, that is

$$P_{cr} = \left((\frac{\pi}{a})^2 + (\frac{\pi}{b})^2\right)^2\left[p_1\left(1 + (\frac{a}{b})^2\right) + p_2(\frac{a}{\pi})^2\right] + k(\frac{a}{\pi})^2 \tag{47}$$

Figure 5 illustrates the variation of the normalized critical load (P_{cr}/f) with size scale (f), where results from all of the three models are presented with and

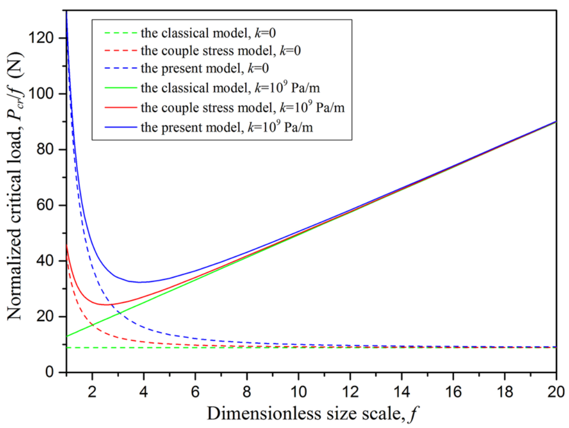

Fig. 5 Normalized critical buckling load with size scale

without elastic medium. The parameters are the same as those in the static problem mentioned above. For the classical model without elastic medium, the normalized critical load (P_{cr}/f) is constant. For the present model and modified couple stress model, it can be seen that the normalized critical load depends on the size scale of the micro-plate from the Fig. 5. The variation trend of the normalized critical load is similar to that of the normalized stiffness. When the plate thickness is greater than 15 times of the material length scale parameter, there is almost no difference between the critical buckling loads from all of the three models.

The variation of the critical buckling load (P_{cr}) with elastic medium parameter (k) is shown in Fig. 6 in which the horizontal axis increases exponentially. When the medium parameter k is small, there are significant differences between the critical buckling

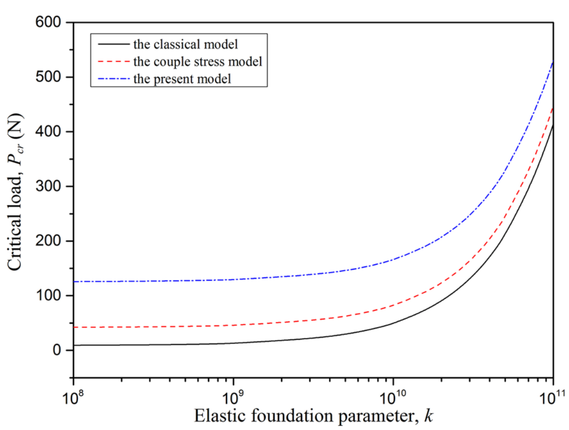

Fig. 6 Critical buckling load with foundation parameter

loads predicted by the three models and the size effect of the micro-plate cannot be neglected. With the increase of the value of the foundation parameter, the relative differences of critical buckling loads predicted from the three models decrease.

5 Free vibration of simply supported size-dependent plate

Finally, the free vibration problem of a simply supported rectangular micro-plate on an elastic foundation is solved. No external force is applied on the structure. The governing equation is expressed as

$$\rho g\ddot{w} - p_1\nabla^6 w + p_2\nabla^4 w + kw = 0 \tag{48}$$

where w is dependent with time scale t. Similar to the procedure of classical model [42], the following Fourier series solutions for $w(x, y, t)$ is employed, which incorporates the spatial and temporal parts.

$$w(x,y,t) = \sum_{m=1}^{\infty}\sum_{n=1}^{\infty} C_{mn}\sin\left(\frac{m\pi x}{a}\right)\sin\left(\frac{n\pi y}{b}\right)e^{i\omega_{mn}t} \tag{49}$$

in which C_{mn} is Fourier coefficient, ω_{mn} is the vibrational frequency, and i is the usual imaginary number defined by $i^2 = -1$. Equation (49) satisfies the boundary conditions in Eq. (37) for any C_{mn}.

By substituting Eq. (49) into Eq. (48), ω_{mn}^2 is obtained as a simple form,

$$\omega_{mn}^2 = \frac{C_1 p_1 + C_2 p_2 + k}{\rho h} \tag{50}$$

The positive solution of ω_{mn} determined from Eq. (50) is the natural frequency of the simply supported plate for different order number m and n.

In the following, the fundamental natural frequency for $m = 1$ and $n = 1$ is considered. The parameters are the same as those in Sect. 3. For comparison purposes, the results from the three models are given in Fig. 7 with and without elastic medium effect. The normalized natural frequency shows similar size-dependent trends with that of the normalized stiffness (Sect. 3) and normalized critical load (Sect. 4). For the classical model without elastic medium, the normalized natural frequency ($f\omega_{11}$) is constant. For the present model and modified couple stress model, it can be seen that the normalized natural frequency depends

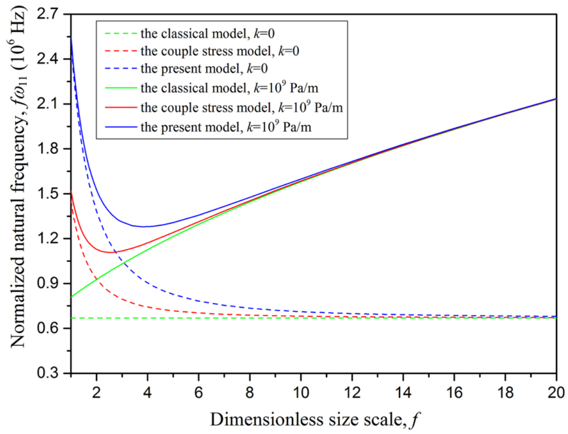

Fig. 7 Normalized natural frequency with size scale

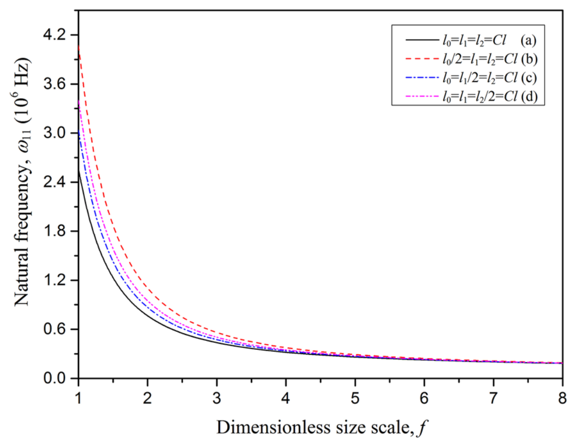

Fig. 9 Effects of different MLSPs on frequency

on the size scale of the micro-plate. When the plate thickness is greater than 20 times of the material length scale parameter, there is almost no difference between the normalized natural frequencies from all of the three models. When the elastic medium (assuming $k = 10^9 Pa/m$) is considered, the normalized natural frequency increases almost linearly for the classical model, but for the present model and the modified couple stress model, the normalized natural frequency decreases and then increases as the size scale increases.

The variation of the natural frequency (ω_{11}) with elastic medium parameter (k) is shown in Fig. 8 in which the horizontal axis increases exponentially. When the medium parameter k is smaller than $10^{11} Pa/m$, there are significant differences between the natural frequencies predicted by the three models. So the size effect of the micro-plate cannot be neglected when the medium parameter k is smaller than $10^{11} Pa/m$. These three models show almost no difference of the natural frequency if the elastic medium parameter k is more than $10^{12} Pa/m$.

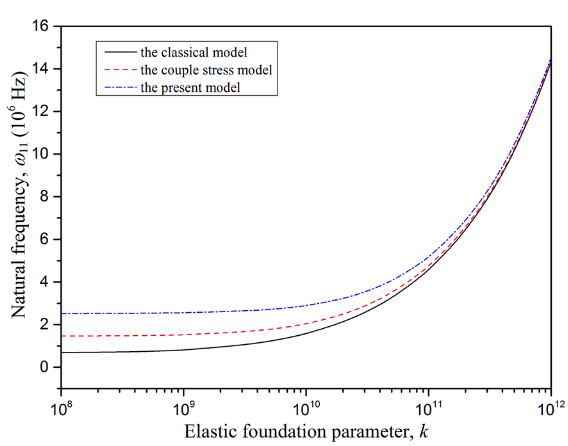

Fig. 8 Natural frequency with foundation parameters

Similar to Fig. 4, the effects of different MLSPs on natural frequency of the plate have been studied as shown in Fig. 9, where the variations of natural frequency with the dimensionless size scale f are plotted for four cases of MLSPs. In Fig. 9, the black solid curve is for the case of $l_0 = l_1 = l_2 = Cl$, the other curves are calculated by doubling one of the three MLSPs, respectively, which is the same as did in Fig. 4. The frequency of case (d) is smaller than that of case (b) and larger than that of case (c). The higher frequency represents the higher stiffness, which results in the smaller deflection, so what shown in Fig. 9 is consistent with what shown in Fig. 4. Therefore, the dilatation gradient plays a more important role than the other two gradients.

6 Concluding remarks

In this paper, an application of a size-dependent Kirchhoff plate resting on elastic medium is presented, and three material length scale parameters are contained in the model. If two (l_0 and l_1) or three (l_0, l_1 and l_2) material length scale parameters are ignored, the model can degenerate to the modified couple stress model and the classical model. The differences between the three models and the influences of elastic medium coefficient on the static bending, buckling and vibration response of a simply supported micro-plate on an elastic medium are discussed in detail.

Numerical results indicate that the normalized stiffness, normalized critical load, and normalized natural frequency exhibit strong size-dependence. The results predicted by the present model are very different from those predicted by the other two reduced models when the plate thickness is on the same order of the material length scale parameter. These size effects are not significant if the thickness of the plate is about 15 times as large as the material length scale parameter. For the case of highly rigid elastic medium, these size effects are also not significant. The study may be helpful to characterize the mechanical properties of micro-plate based structures that can be modeled as resting on elastic medium.

Acknowledgments The work is supported by the National Natural Science Foundation of China (Grant Nos. 11202117, 51422904, 51379112 and 11272186), Natural Science Fund of Shandong Province (BS2012ZZ006) and the Fundamental Research Funds of Shandong University (Grant No. 2015JX003).

References

1. Batra RC, Porfiri M, Spinello D (2007) Review of modeling electrostatically actuated microelectromechanical systems. Smart Mater Struct 16:R23–R31
2. Chasiotis I, Knauss WG (2003) The mechanical strength of polysilicon films: part 2. Size effects associated with elliptical and circular perforations. J Mech Phys Solids 51:1551–1572
3. Fleck NA, Muller GM, Ashby MF, Hutchinson JW (1994) Strain gradient plasticity: theory and experiment. Acta Metall Mater 42:475–487
4. Poole WJ, Ashby MF, Fleck NA (1996) Micro-hardness of annealed and work-hardened copper polycrystals. Scr Mater 34:559–564
5. McFarland AW, Colton JS (2005) Role of material microstructure in plate stiffness with relevance to micro-cantilever sensors. J Micromech Microeng 15:1060–1067
6. Vardoulakis I, Exadaktylos G, Kourkoulis SK (1998) Bending of marble with intrinsic length scales: a gradient theory with surface energy and size effects. J de physique IV 8:399–406
7. Nix WD (1989) Mechanical properties of thin films. Metall Trans A Phys Metall Mater Sci 20:2217–2245
8. Lam DCC, Yang F, Chong ACM, Wang J, Tong P (2003) Experiments and theory in strain gradient elasticity. J Mech Phys Solids 51:1477–1508
9. Papargyri-Beskou S, Beskos DE (2008) Static, stability and dynamic analysis of gradient elastic flexural Kirchhoff plates. Arch Appl Mech 78:625–635
10. Papargyri-Beskou S, Tsepoura KG, Polyzos D, Beskos DE (2003) Bending and stability analysis of gradient elastic beams. Int J Solids Struct 40:385–400
11. Batra RC (1987) The initiation and growth of, and the interaction among, adiabatic shear bands in simple and dipolar materials. Int J Plast 3:75–89
12. Wang B, Zhao J, Zhou S (2010) A micro scale Timoshenko beam model based on strain gradient elasticity theory. Eur J Mech A Solids 29:591–599
13. Reddy JN (2007) Nonlocal theories for bending, buckling and vibration of beams. Int J Eng Sci 45:288–307
14. Kong S, Zhou S, Nie Z, Wang K (2009) Static and dynamic analysis of micro beams based on strain gradient elasticity theory. Int J Eng Sci 47:487–498
15. Papargyri-Beskou S, Giannakopoulos AE, Beskos DE (2010) Variational analysis of gradient elastic flexural plates under static loading. Int J Solids Struct 47:2755–2766
16. Ariman T (1968) On circular micropolar plates. Ing Arch 37:156–160
17. Ariman T (1968) Some problems in bending of micropolar plates. I, II(Bending of micropolar plates using differential equations, considering transverse displacement and micro-rotation vector). Acad Polonaise des Sci Bull serie des Sci Tech 16:535–539
18. Mindlin RD (1964) Micro-structure in linear elasticity. Arch Ration Mech Anal 16:51–78
19. Papargyri-Beskou S, Beskos DE (2009) Stability analysis of gradient elastic circular cylindrical thin shells. Int J Eng Sci 47:1379–1385
20. Vavva MG, Protopappas VC, Gergidis LN, Charalambopoulos A, Fotiadis DI, Polyzos D (2009) Velocity dispersion of guided waves propagating in a free gradient elastic plate: Application to cortical bone. J Acoust Soc Am 125:3414–3427
21. Lazopoulos KA (2004) On the gradient strain elasticity theory of plates. Eur J Mech A Solids 23:843–852
22. Lazopoulos KA (2009) On bending of strain gradient elastic micro-plates. Mech Res Commun 36:777–783
23. Hoffman O (1964) On bending of thin elastic plates in the presence of couple stresses. J Appl Mech 31:706–707
24. Ellis RW, Smith CW (1967) A thin-plate analysis and experimental evaluation of couple-stress effects. Exp Mech 7:372–380
25. Tsiatas GC (2009) A new Kirchhoff plate model based on a modified couple stress theory. Int J Solids Struct 46:2757–2764
26. Altan B, Aifantis E (1997) On some aspects in the special theory of gradient elasticity. J Mech Behav Mater 8:231–282
27. Lazopoulos KA, Alnefaie KA, Abu-Hamdeh NH, Aifantis EC (2014) The GRADELA plates and shells. Shell Struct Theory Appl 3:121–124
28. Aifantis EC (2011) On the gradient approach—relation to Eringen's nonlocal theory. Int J Eng Sci 49:1367–1377
29. Aifantis EC (1992) On the role of gradients in the localization of deformation and fracture. Int J Eng Sci 30:1279–1299
30. Mindlin RD (1965) Second gradient of strain and surface-tension in linear elasticity. Int J Solids Struct 1:417–438
31. Yang F, Chong ACM, Lam DCC, Tong P (2002) Couple stress based strain gradient theory for elasticity. Int J Solids Struct 39:2731–2743

32. Fleck NA, Hutchinson JW (1993) A phenomenological theory for strain gradient effects in plasticity. J Mech Phys Solids 41:1825–1857
33. Shu JY, Fleck NA (1998) The prediction of a size effect in microindentation. Int J Solids Struct 35:1363–1383
34. Wang B, Zhou S, Zhao J, Chen X (2011) A size-dependent Kirchhoff micro-plate model based on strain gradient elasticity theory. Eur J Mech A Solids 30:517–524
35. Ferreira AJ, Castro LM, Bertoluzza S (2011) Analysis of plates on Winkler foundation by wavelet collocation. Meccanica 46:865–873
36. Roque C, Rodrigues J, Ferreira A (2012) Analysis of thick plates by local radial basis functions-finite differences method. Meccanica 47:1157–1171
37. Yas M, Jodaei A, Irandoust S, Aghdam MN (2012) Three-dimensional free vibration analysis of functionally graded piezoelectric annular plates on elastic foundations. Meccanica 47:1401–1423
38. Kumar Y, Lal R (2012) Vibrations of nonhomogeneous orthotropic rectangular plates with bilinear thickness variation resting on Winkler foundation. Meccanica 47:893–915
39. Malekzadeh P, Haghighi MG, Beni AA (2012) Buckling analysis of functionally graded arbitrary straight-sided quadrilateral plates on elastic foundations. Meccanica 47:321–333
40. Akgoz B, Civalek O (2013) Modeling and analysis of micro-sized plates resting on elastic medium using the modified couple stress theory. Meccanica 48:863–873
41. Dym CL, Shames IH (1973) Solid mechanics: a variational approach. McGraw-Hill Inc., New York
42. Ventsel E, Krauthammer T (2001) Thin plates and shells: theory: analysis, and applications. CRC Press, New York
43. Sciarra G, Vidoli S (2013) Asymptotic fracture modes in strain-gradient elasticity: size effects and characteristic lengths for isotropic materials. J Elast 113:27–53